Conductive Molecular Crystals. Structural, Magnetic, and Charge-Transport Properties of (5,10,15,20-Tetramethylporphyrinato)nickel(II) Iodide

Laurel J. Pace, Jens Martinsen, Abraham Ulman, Brian M. Hoffman,* and James A. Ibers*

Contribution from the Department of Chemistry and Materials Research Center, Northwestern University, Evanston, Illinois 60201. *Received August 16, 1982*

Abstract: (5,10,15,20-Tetramethylporphyrinato)nickel(II), Ni(tmp), has been partially oxidized by reaction with iodine. We report the structural, magnetic, and charge-transport properties of single crystals of the resulting compound, Ni(tmp)I. The compound crystallizes in space group D_{4h}^4-$P4/nnc$ of the tetragonal system with four formula units in a cell of dimensions a = 16.610 (15) Å and c = 6.932 (7) Å at 114 K. Full-matrix least-squares refinement of 69 variables gives a final value for the R index on F^2 of 0.079 for 1418 observations. The structure consists of S_4-ruffled Ni(tmp) molecules, stacked metal-over-metal, with a Ni–Ni spacing along the stack of 3.466 (3) Å. Adjacent Ni(tmp) units in the unit cell are staggered by 37°. Severely disordered chains of iodine are located in channels surrounding the Ni(tmp) stacks. The iodine is identified as I_3^- from diffuse X-ray scattering and resonance Raman spectroscopy. Splitting of the I_3^- bands in the resonance Raman spectrum becomes evident at low temperature. Single-crystal room-temperature conductivity along the needle axis averages 110 Ω^{-1} cm^{-1}, slightly less than that of large-ring porphyrinic conductors. The temperature dependence of the conductivity of Ni(tmp)I is metal-like above 115 K and activated at lower temperatures. Single-crystal EPR studies indicate that the oxidation of the Ni(tmp) moiety is ligand centered. The magnetic susceptibility is metal-like, being temperature independent above 28 K but anomalously high ($\sim^1/_3$ spin/macrocycle), indicative of enhanced Coulomb correlations. This susceptibility enhancement may arise from the mixing in of a magnetic triplet state that is available because of the electronic structure of small porphyrinic macrocycles. The susceptibility decreases sharply as the temperature is lowered below 28 K.

We have been preparing stacked molecular conductors having porphyrinic metallomacrocycles as building blocks in order to probe the relationship between molecular and solid-state properties.[1-6] One example of this approach is our study of a series of iodinated large-ring metallomacrocycle compounds Ni(pc)I,[2,7] Ni(tatbp)I,[3] and Ni(tbp)I.[4] These isostructural and isoionic compounds exhibit comparably high electrical conductivities at room temperature. However, the details of the temperature dependence of the conductivity and the nature of the charge carriers differ from compound to compound, and these differences can be understood in terms of the differences in the electronic structures of the parent metallomacrocycles. We present here the structural, magnetic, and charge-transport properties of single crystals of Ni(tmp)I, a highly conducting compound obtained by the partial oxidation with iodine of the small-ring molecule (5,10,15,20-tetramethylporphyrinato)nickel(II), Ni(tmp). The only previous report of a partially oxidized small-ring porphyrin system has been a study of polycrystalline samples of M(oep)I_x, M = "H_2", Ni, Cu; $x \leq 5.8$.[5,7]

The comparison of systems based on metallomacrocycles having conjugated frameworks of different sizes allows us to address one of the broad problems in the study of quasi-one-dimensional molecular conductors,[8] that of defining the relative importance of the interactions that tend to delocalize the charge carriers along a conducting molecular chain and of the Coulomb correlations (repulsions) between carriers that tend to localize them.[9] The former are strongly dependent on the orientation of and spacing between the units on the conducting stack, while the latter more closely reflect molecular properties such as size, polarizability, and extent of conjugation. We find that Ni(tmp)I, whose properties are similar to those of some TTF-based quasi-one-dimensional conductors,[10] falls between two large-ring systems, Ni(tbp)I[4] and Ni(omtbp)$I_{1.08}$,[6] in a series of complexes in which correlation effects are of increasingly greater relative importance. We surmise that the increased correlation effects arise both from the less extensive conjugated framework in the small-ring macrocycle and from well-defined features of the crystal structure, namely increasing intermolecular spacing in the conducting stack as measured by the Ni–Ni separation.

Experimental Section

Preparation of Ni(tmp)I. Ni(tmp) was prepared as described previously.[11] Single crystals of Ni(tmp)I were grown in an H-tube by dif-

(1) (a) Hoffman, B. M.; Phillips, T. E.; Schramm, C. J.; Wright, S. K. In "Molecular Metals"; Hatfield, W. E., Ed.; Plenum Press: New York, 1979; pp 393-398. (b) Euler, W. B.; Martinsen, J.; Pace, L. J.; Ibers, J. A.; Hoffman, B. M. *Mol. Cryst. Liq. Cryst.* **1982**, *77*, 949-960. (c) Ibers, J. A.; Pace, L. J.; Martinsen, J.; Hoffman, B. M. *Struct. Bonding (Berlin)* **1982**, *50*, 1-55. (d) Hoffman, B. M.; Martinsen, J.; Pace, L. J.; Ibers, J. A. In "Extended Linear Chain Complexes"; Miller, J. S., Ed.; Plenum Press: New York, 1983; Vol. 3, pp 459-550. (e) Hoffman, B. M.; Ibers, J. A. *Acc. Chem. Res.* **1983**, *16*, 15-21.

(2) (a) Peterson, J. L.; Schramm, C. J.; Stojakovic, D. R.; Hoffman, B. M.; Marks, T. J. *J. Am Chem. Soc.* **1977**, *99*, 286-288. (b) Schramm, C. J.; Stojakovic, D. R.; Hoffman, B. M.; Marks, T. J. *Science (Washington, D.C.)* **1978**, *200*, 47-48. (c) Schramm, C. J.; Scaringe, R. P.; Stojakovic, D. R.; Hoffman, B. M.; Ibers, J. A.; Marks, T. J. *J. Am. Chem. Soc.* **1980**, *102*, 6702-6713. (d) Martinsen, J.; Greene, R. L.; Palmer, S. M.; Hoffman, B. M. *Ibid.* **1983**, *105*, 677-678.

(3) Euler, W. B.; Hoffman, B. M., manuscript in preparation.

(4) Martinsen, J.; Pace, L. J.; Phillips, T. E.; Hoffman, B. M.; Ibers, J. A. *J. Am. Chem. Soc.* **1982**, *104*, 83-91.

(5) Wright, S. K.; Schramm, C. J.; Phillips, T. E.; Scholler, D. M.; Hoffman, B. M. *Synth. Met.* **1979**, *1*, 43-51.

(6) (a) Phillips, T. E.; Hoffman, B. M. *J. Am. Chem. Soc.* **1977**, *99*, 7734-7736. (b) Phillips, T. E.; Scaringe, R. P.; Hoffman, B. M.; Ibers, J. A. *Ibid.* **1980**, *102*, 3435-3444. (c) Hoffman, B. M.; Phillips, T. E.; Soos, Z. G. *Solid State Commun.* **1980**, *33*, 51-54.

(7) Abbreviations used: tmp, 5,10,15,20-tetramethylporphyrinato; tbp, tetrabenzoporphyrinato; tatbp, triazatetrabenzoporphyrinato; omtbp, 1,4,5,8,9,12,13,16-octamethyltetrabenzoporphyrinato; pc, phthalocyaninato; oep, 2,3,7,8,12,13,17,18-octaethylporphyrinato; deut, 2,7,12,18-tetramethyl-3,8,-diacetyl-13,17-bis(2′-carboxyethyl)porphyrinato; dpg, diphenylglyoximato; bqd, benzoquinonedioximato; NMP, *N*-methylphenazinium; TCNQ, 7,7,8,8-tetracyano-*p*-quinodimethane; TTF, tetrathiafulvalene; TMTTF, tetramethyltetrathiafulvalene; TTT, tetrathiatetracene; $DIPSPh_4$, tetraphenyldithiapyranilidene.

(8) (a) Miller, J. S.; Epstein, A. J., Eds. *Ann. N.Y. Acad. Sci.* **1978**, *313*. (b) Keller, H. J., Ed. "Chemistry and Physics of One-Dimensional Metals"; Plenum Press: New York, 1977. (c) Miller, J. S.; Epstein, A. J. *Prog. Inorg. Chem.* **1976**, *20*, 1-151. (d) Hatfield, W. E., Ed. "Molecular Metals"; Plenum Press: New York, 1979. (e) Barisic, S.; Bjelis, A.; Cooper, J. R.; Leontic, B. *Lect. Notes Phys.* **1979**, *95*. (f) *Ibid.* *96*. (g) Devreese, J. T.; Evrard, R. P.; Van Doren, V. E., Eds. "Highly Conducting One-Dimensional Solids"; Plenum Press: New York, 1979. (h) *Mol. Cryst. Liq. Cryst.* **1982**, *77*.

(9) (a) Torrance, J. B.; Silverman, B. D. *Phys. Rev. B: Condens. Matter* **1977**, *15*, 798-809. (b) Torrance, J. B. *Ibid.* **1978**, *17*, 3099-3112. (c) Torrance, J. B. *Acc. Chem. Res.* **1979**, *12*, 79-86. (d) Torrance, J. B., in ref 8b; pp 137-191. (e) Heeger, A. J., in ref 8g; pp 69-145.

(10) Delhaes, P.; Coulon, C.; Amiell, J.; Flandrois, S.; Toreilles, E.; Fabre, J. M.; Giral, L. *Mol. Cryst. Liq. Cryst.* **1979**, *50*, 43-58.

0002-7863/83/1505-2612$01.50/0

Table I. Summary of Crystal Data and Intensity Collection

compd	Ni(tmp)I
formula	$C_{24}H_{20}IN_4Ni$
formula wt, amu	550.07
space group	D^4_{4h}-$P4/nnc$
cell: a, Å	16.610 (15)
c, Å	6.932 (7)
V, Å^3	1913
Z	4
density: calcd, g cm^{-3}	1.910 (114 K)[a]
obsd,[b] g cm^{-3}	1.88 (4) (298 K)
cryst shape	needle of rectangular cross section bounded by faces of the forms {110}, {001} with separations of 0.064, 0.057, 0.680 mm, respectively
cryst volume, mm^3	0.00248
radiatn	graphite-monochromated Mo Kα
	λ(Mo Kα_1) = 0.70930 Å
μ	26.4 cm^{-1}
transmissn factors	0.85–0.87
take-off angle, deg	3.0
receiving aperture	5.0 mm high × 5.0 mm wide 34 cm from crystal
scan speed, deg min^{-1}	1
scan width	0.85° below Kα_1 to 0.85° above Kα_2
background counts	40-s total with rescan option[c]
data collected	$h,k,l \geq 0$
	$3.4° \leq 2\theta \leq 60°$
unique data	1418
unique data with $\|F_o\|^2 \geq 3\sigma(F_o^2)$	655
final no. of variables	69
final cycle on F_o^2, R	0.079
R_w	0.129
F_o for data with $F_o^2 > 3\sigma(F_o^2)$, R	0.047
R_w	0.055
error in obsd unit wt	1.21e^2

[a] The low-temperature system is based on a design by J. C. Huffman (Ph.D. Thesis, Indiana University, 1974). [b] Flotation in $ZnBr_2/H_2O$. [c] The diffractometer was run under the disk-oriented Vanderbilt system (Lenhert, P. G. *J. Appl. Crystallogr.* 1975, *8*, 568–570).

fusing together benzene solutions of Ni(tmp) and I_2. The small, dark green needles begin to lose iodine when heated above 70 °C but are stable at room temperature. Elemental analyses were carried out by Galbraith Laboratories, Inc., Knoxville, TN, and are consistent with a Ni(tmp):I ratio of 1:1. Anal. Calcd for $C_{24}H_{20}IN_4Ni$: C, 52.41; H, 3.66; I, 23.07; N, 10.19; Ni, 10.67. Found: C, 52.55; H, 3.59; I, 22.97; N, 10.22; Ni, 10.80.

Resonance Raman Measurements. Resonance Raman spectra were recorded on a spectrometer described previously.[12] A 180° backscattering geometry was used to illuminate solid samples that were contained in spinning, 5-mm Pyrex tubes. Low temperature (~10 K)[13] spectra were obtained on samples that were sealed in Pyrex tubes under a helium atmosphere and cooled in an apparatus described elsewhere.[14]

X-ray Diffraction Study of Ni(tmp)I. On the basis of Weissenberg and precession photographs, single crystals of Ni(tmp)I were assigned to Laue group $4/mmm$ of the tetragonal system. The systematic absences ($hk0$, $h + k$ odd; $0kl$, $k + l$ odd; and hhl, l odd) are consistent with space group D^4_{4h}-$P4/nnc$. The cell constants of a = 16.610 (15) Å and c = 6.932 (7) Å at 114 K were determined by a least-squares refinement of the setting angles of 14 reflections that had been centered on a FACS-I diffractometer with the use of graphite-monochromated Mo Kα radiation. Intensity data were collected at 114 (2) K by the θ–2θ technique[15] and

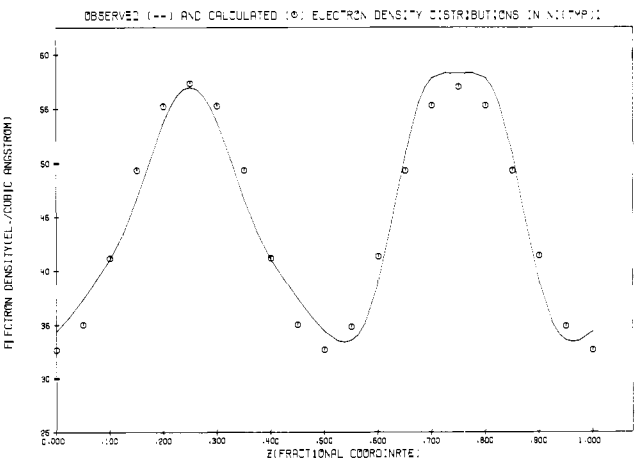

Figure 1. Plot of the observed (–) and calculated (O) electron density along the line $^1/_4$, $^1/_4$, z (the iodine channel). The calculated line is a sine-squared curve.

were processed by methods standard in this laboratory.[16,17] No absorption correction was made since sample calculations, based on a linear absorption coefficient of 26.4 cm^{-1}, resulted in transmission factors that ranged from 0.85 to 0.87. Of the 3218 reflections collected, 1418 are unique and of these 655 have $F_o^2 > 3\sigma(F_o^2)$. Crystal data and experimental details are given in Table I.

In addition to Bragg scattering, oscillation and precession photographs showed diffuse scattering localized in planes perpendicular to the c axis. This type of diffuse scattering pattern is commonly observed in systems that contain one-dimensionally disordered polyiodide chains.[2c,4,6b,18–24] To augment the photographic data, the diffuse scattering was measured by X-ray counter techniques with the same crystal and experimental setup used for measuring the Bragg scattering. Reciprocal space was sampled for 1000 s every 0.05° in 2θ from 3.0 to 40.4° along a line perpendicular to the diffuse planes. Two parallel scans were taken to ensure that no Bragg scattering had been accidentally measured. Combination of data from both the photographs and diffractometer scans results in a diffuse scattering pattern of nine lines. Seven of these lines correspond to the $l' = 1$–7 lines of a superlattice with spacing c' of 9.64 (9) Å, a value well within the range of 9.4–9.8 Å expected for systems that contain chains of triiodide ions.[2c,4,18–22] The iodine superlattice is incommensurate with the Bragg lattice ($c' = 1.39c$), a feature that has been found in the metalloporphyrin system Ni(omtbp)$I_{1.08}$[6b] and in several organic iodide systems.[20–22,23a]

An origin-removed, sharpened Patterson map indicated that the positions of the iodine atoms are 0, $\pm^1/_2$, $\pm^1/_4$ from those of the nickel atoms. With this constraint and with four formula units in the cell possible special positions for the nickel atom in $P4/nnc$ (unit cell origin at $\bar{1}$) are (4d) with $\bar{4}$ symmetry or (2a) and (2b) both with 42 symmetry. The iodine-to-porphyrin vectors were used to determine the correct orientation of the porphyrin ring and to establish that the nickel atom is on the $\bar{4}$ site. Thus, the asymmetric unit consists of one-quarter of a Ni(tmp) molecule centered at special position (4d) and one-eighth of an

(11) (a) Ulman, A.; Gallucci, J.; Fisher, D.; Ibers, J. A. *J. Am. Chem. Soc.* **1980**, *102*, 6852–6854. (b) Ulman, A.; Fisher, D.; Ibers, J. A. *J. Heterocycl. Chem.* **1982**, *19*, 409–413.
(12) Shriver, D .F.; Dunn, J. B. R. *Appl. Spectrosc.* **1974**, *28*, 319–323.
(13) The actual sample temperature may be higher than the 10 K reading from the thermocouple because of local heating of the sample by the laser beam.
(14) Cooper, C. B. Ph.D. Thesis, Northwestern University, 1978.
(15) See, for example: Waters, J. M.; Ibers, J. A. *Inorg. Chem.* **1977**, *16*, 3273–3277.
(16) Corfield, P W. R.; Doedens, R. J.; Ibers, J. A. *Inorg. Chem.* **1967**, *6*, 197–204.
(17) A value of $p = 0.04$[16] was used in the estimation of standard deviations. In addition to local programs, other programs for the Northwestern CDC 6600 computer include Zalkin's FORDAP Fourier summation program, Johnson's ORTEP II thermal ellipsoid plotting program, and Busing's and Levy's ORFFE error function program. Our full-matrix least-squares program, NUCLS, in its nongroup form closely resembles the Busing-Levy ORFLS program.
(18) Huml, K. *Acta Crystallogr.* **1967**, *22*, 29–32.
(19) Endres, H.; Keller, H. J.; Megnamisi-Belombe, M.; Moroni, W.; Pritzkow, H.; Weiss, J.; Comès, R. *Acta Crystallogr., Sect. A* **1976**, *A32*, 954–957.
(20) Endres, H.; Harms, R.; Keller, H. J.; Moroni, W.; Nothe, D.; Vartanian, M. H.; Soos, Z. G. *J. Phys. Chem. Solids* **1979**, *40*, 591–596.
(21) (a) Smith, D. L.; Luss, H. R. *Acta Crystallogr., Sect. B* **1977**, *B33*, 1744–1749. (b) Hilti, B.; Mayer, C. W. *Helv. Chim. Acta* **1978**, *61*, 501–511.
(22) (a) Isett, L. C.; Reynolds, G. A.; Schneider, E. M.; Perlstein, J. H. *Solid State Commun.* **1979**, *30*, 1–6. (b) Luss, H. R.; Smith, D. L. *Acta Crystallogr., Sect. B* **1980**, *B36*, 1580–1588.
(23) (a) Delhaes, P.; Coulon, C.; Flandrois, S.; Hilti, B.; Mayer, C. W.; Rihs, G.; Rivory, J. *J. Chem. Phys.* **1980**, *73*, 1453–1463. (b) Scaringe, R. P.; Pace, L. J.; Ibers, J. A. *Acta Crystallogr., Sect. A* **1982**, *A38*, 608–611.
(24) Brown, L. D.; Kalina, D. W.; McClure, M. S.; Schultz, S.; Ruby, S. L.; Ibers, J. A.; Kannewurf, C. R.; Marks, T. J. *J. Am. Chem. Soc.* **1979**, *101*, 2937–2947.

Table II. Positional and Thermal Parameters for the Atoms of NI(tmp)I

ATOM	X[A]	Y	Z	P11 OR P,A[2]	P22	P33	P12	P13	P23
NI	1/4	3/4	0	6.09(18)	6.09	57.3(18)	0	0	0
N	0.19800(16)	0.64572(17)	0.01463(59)	6.95(98)	7.84(98)	69.1(71)	0.06(73)	-3.6(27)	-1.7(25)
C(1)	0.23344(20)	0.57139(20)	0.00626(82)	12.5(15)	6.2(11)	42.8(69)	-0.73(79)	-1.6(32)	0.3(31)
C(2)	0.17522(24)	0.50916(23)	0.04698(62)	14.9(15)	6.3(13)	94.(10)	-4.0(10)	-0.8(29)	5.2(27)
C(3)	0.10432(24)	0.54517(24)	0.07893(62)	11.6(14)	8.0(13)	77.1(82)	-3.0(10)	-1.7(28)	1.9(29)
C(4)	0.11698(25)	0.63077(24)	0.05358(54)	10.1(13)	13.2(15)	43.7(73)	-3.8(10)	-3.1(26)	-2.1(26)
C(5)	0.05554(23)	0.68845(24)	0.04100(58)	9.1(13)	12.8(14)	50.1(91)	-1.5(10)	-1.9(25)	-7.4(26)
C(6)	-0.03104(25)	0.66004(25)	0.06234(66)	9.3(14)	13.7(14)	87.3(92)	-2.2(11)	3.5(28)	-2.3(29)
H1C(2)	0.186	0.452	0.051	2.3					
H1C(3)	0.055	0.520	0.111	2.7					
H1C(6)	-0.065	0.705	0.091	2.3					
H2C(6)	-0.050	0.636	-0.055	2.3					
H3C(6)	-0.036	0.622	0.164	2.3					

[a] Estimated standard deviations in the least significant figure(s) are given in parentheses in this table. [b] The form of the anisotropic thermal ellipsoid is: $\exp[-(\beta_{11}h^2 + \beta_{22}k^2 + \beta_{33}l^2 + 2\beta_{12}hk + 2\beta_{13}hl + 2\beta_{23}kl)]$. The quantities given in the table are the thermal coefficients $\times 10^4$.

iodine atom centered at each of the special positions (2a) and (2b).

Initial refinements were carried out on $|F_o|$, using the 655 reflections having $F_o^2 \geq 3\sigma(F_o^2)$. The function minimized was $\sum w(|F_o| - |F_c|)^2$, where $|F_o|$ and $|F_c|$ are the observed and calculated structure amplitudes and the weight w is $4F_o^2/(\sigma^2(F_o^2))$. The positions of five of the seven non-hydrogen atoms of the porphyrin ring were located from the Patterson map, and the two remaining atoms were located in a subsequent difference electron density map. A refinement of all of the atoms in the asymmetric unit resulted in high R indices ($\sim$0.45), and the isotropic thermal parameters of several atoms of the porphyrin ring were nonpositive definite. The problem was assumed to be the result of iodine disorder, and lower R indices ($\sim$0.10) and an improved light-atom model were obtained when refinement was restricted to those reflections that are not influenced by the disordered iodine atoms ($hk0$ and $h + k + l \neq 2n$ reflections). Structure factors were calculated with no contribution from iodine and an ensuing difference map revealed that the distribution of electron density in the iodine channel ($^1/_4$, $^1/_4$, z) consisted of two broad peaks, differing markedly in shape, with maxima at $z = {}^1/_4$ and $z = {}^3/_4$ (special positions (2a) and (2b), respectively) and minima at approximately $z = 0$ and $z = {}^1/_2$. At this point we decided to use a statistical distribution of electron density[23b] to model the observed distribution, an approach that had been successful in solving a similar disorder problem in the structure of Ni(omtbp)$I_{1.08}$.[6b] We found that a sine-squared distribution of the form

$$\rho(z) = \frac{4\Omega}{\alpha_1 + 2\alpha_2}(\alpha_1 \sin^2 2\pi z + \alpha_2) \qquad (1)$$

gives an excellent fit (Figure 1) to the data. Here $\rho(z)$ is the normalized probability of finding an atom between z and $z + dz$, Ω is related to the number of iodine atoms in the unit cell, α_1 is the amplitude of the distribution, and α_2 is the height of the distribution above 0. To avoid correlation problems the two distributions centered at $^1/_4$, $^1/_4$, $^1/_4$ and $^1/_4$, $^1/_4$, $^3/_4$ were constrained to be identical.

The sine-squared distribution was incorporated into the least-squares program, and several cycles of refinement, first with variable isotropic thermal parameters and then with variable anisotropic thermal parameters, resulted in values of 0.051 and 0.061 for R and R_w, respectively. All hydrogen atom positions were located in a difference electron density map, and their idealized positions (C–H = 0.95 Å) were used and were not varied. The isotropic thermal parameter of a hydrogen atom was assumed to be 1.0 Å^2 greater than that of the carbon atom to which it is attached. Two cycles of refinement were carried out on F_o^2 using all 1418 reflections to yield final values of R and R_w on F^2 of 0.079 and 0.129, respectively. The values for R and R_w on F_o for the reflections having $F_o^2 > 3\sigma(F_o^2)$ are 0.047 and 0.055, respectively. The highest peak in the final difference electron density map (3.0 e/Å^3) is located between the maxima of the iodine distribution and is about 5% of the height of an iodine peak. Aside from a slightly smaller peak (2.7 e/Å^3) located near one of the maxima of the iodine distribution and two peaks between the nickel atoms (1.2, 1.7 e/Å^3), the difference map has no other outstanding features. The final positional and thermal parameters are given in Table II, and the root-mean-square amplitudes of vibration are in Table III.[25] A listing of observed and calculated structure amplitudes is also available.[25] In this listing an entry with a negative value for F_o symbolizes a reflection having $F_o^2 < 0$. From the refinement of the sine-squared distribution, the occupancy of the iodine atom was found to correspond to 1.109 (5) iodine atoms per Ni(tmp) molecule. Attempts to constrain the Ni(tmp):I ratio to be exactly 1:1 resulted in higher R indices ($R = 0.117$, $R_w = 0.156$ on F_o^2) and poor agreement between $|F_o|$ and $|F_c|$ for several $hk0$ reflections.

Magnetic Measurements. Powder and single-crystal electron paramagnetic resonance spectra were obtained on a modified Varian E-4 X-band spectrometer with 100-kHz field modulation as described previously.[6b] Temperature-dependent EPR measurements in the range 95–295 K were carried out with the sample cooled by liquid nitrogen boil-off gas. Measurements in the range 10–160 K were carried out in an Air Products LTD-3 cryostat system with the use of liquid helium; the temperature was monitored with a chromel Au–Fe thermocouple.

Integrated EPR intensities were obtained from numerical double integrations carried out on a Fabritek Model 1074 instrument computer. Absolute EPR intensities were determined at room temperature with the use of DPPH (n = 0.89 spin/molecule)[26] dispersed in KBr as the standard. The static susceptibility, χ, was measured by the Faraday technique with $Hg(Co(SCN)_4)$[27] as the standard. Variable-temperature measurements (77–300 K) were made by cooling the sample with liquid nitrogen and allowing it to warm slowly to room temperature.

Electrical Conductivity Measurements. The electrical conductivity along the needle (c) axis of single crystals of Ni(tmp)I was measured at 27 Hz by a four-probe ac phase-locked technique.[28] The crystal was mounted on four thin (8μm) graphite fibers that had been connected to four of the aluminum wires in an integrated circuit header. All electrical contacts were made with a conductive palladium paint prepared as previously described.[6b] The conductivity of the crystal was calculated from the relation $\sigma = L/RA$, where σ is the conductivity (in Ω^{-1} cm^{-1}), L is the separation between the two inner contacts, R is the resistance between these two contacts, and A is the cross-sectional area. The sampling current used was 10 μA, although ohmic behavior was verified with currents ranging from 0.1 to 100 μA. For the tetragonal needles of Ni(tmp)I, A was typically 1.7×10^{-5} cm^2 and L ranged from 0.03 to 0.09 cm. The uncertainties in the measurement of sample dimensions are estimated[6b] to cause an uncertainty in the absolute conductivity of $\Delta\sigma/\sigma = \pm 0.2$. The small dimensions of the crystal preclude the possibility of conductivity measurements perpendicular to the needle axis.

Variable-temperature measurements were carried out with the sample cooled by either liquid nitrogen (95–295 K) or liquid helium (35–295 K) boil-off gas. The sample temperature was monitored with a copper–constantan thermocouple located in the sample holder. The temperature dependence of the electrical conductivity was measured with both increasing and decreasing temperature to check for hysteresis; cooling and warming rates were typically 1.5 K per min.

Results

Description of the Packing. A stereoview of the packing in the unit cell of Ni(tmp)I is shown in Figure 2. The S_4-ruffled Ni(tmp) molecules are stacked metal-over-metal such that their mean molecular planes are perpendicular to the crystallographic c axis. Chains of iodine atoms, parallel to the c axis, are located in channels created by the methyl and pyrrole hydrogen atoms of the porphyrin. The Ni–Ni separation of 3.466 (3) Å ($c/2$) is

(25) Supplementary material.

(26) Duffy, W., Jr.; Strandburg, D. L. *J. Chem. Phys.* **1967**, *46*, 456–464.
(27) Figgis, B. N.; Nyholm, R. S. *J. Chem. Soc.* **1958**, 4190–4191.
(28) Phillips, T. E.; Anderson, J. R.; Schramm, C. J.; Hoffman, B. M. *Rev. Sci. Instrum.* **1979**, *50*, 263–265.

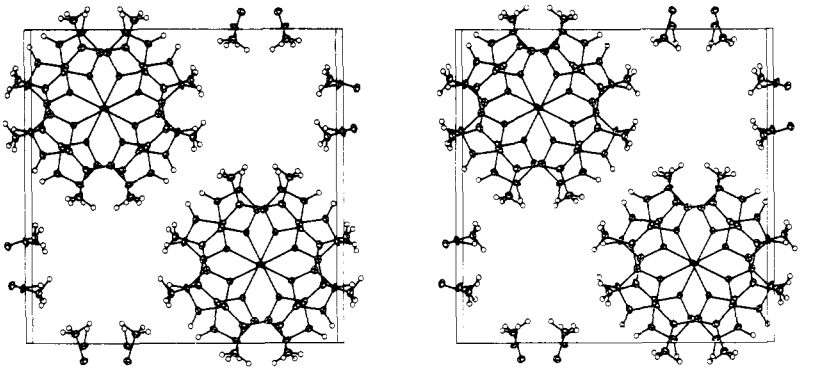

Figure 2. Stereoview of the unit cell of Ni(tmp)I as viewed down the z axis with the x axis horizontal and the y axis vertical. The maxima of the iodine distribution are indicated by dots in the iodine channel. Methyl groups and fragments of pyrrole rings of some of the Ni(tmp) molecules have been included to show the packing around the iodine channels. Vibrational ellipsoids are drawn at the 50% probability level, except those of the hydrogen atoms which are drawn arbitrarily small.

Table IV. Selected Distances (Å) and Angles (deg) in Ni(tmp)I

atoms	type[a]	distance/angle	atoms	type	distance/angle
		Distances			
Ni-N	Ni-N	1.938 (8)	C(2)-C(3)	C_b-C_b	1.339 (6)
N-C(1)		1.369 (5)	C(1)-C(5)		1.396 (6)
N-C(4)		1.395 (5)	C(4)-C(5)		1.380 (6)
av[b]	N-C_a	1.381 (18)	av	C_a-C_m	1.388 (11)
C(1)-C(2)		1.443 (5)	C(5)-C(6)	C_m-C_{Me}	1.511 (6)
C(3)-C(4)		1.448 (5)			
av	C_a-C_b	1.446 (5)	Ni-C(5)	Ni-C_m	3.410 (5)
		Angles			
N-Ni-N	N-Ni-N	90.16 (1)	C(1)-C(2)-C(3)		107.5 (3)
			C(2)-C(3)-C(4)		106.9 (4)
Ni-N-C(1)		127.7 (2)	av	C_a-C_b-C_b	107.2 (5)
Ni-N-C(4)		126.8 (2)			
av	Ni-N-C_a	127.3 (7)	C(2)-C(1)-C(5)		123.3 (3)
			C(3)-C(4)-C(5)		123.9 (4)
C(1)-N-C(4)	C_a-N-C_a	105.2 (3)	av	C_b-C_a-C_m	123.6 (4)
N-C(1)-C(2)		110.5 (3)	C(1)-C(5)-C(4)	C_a-C_m-C_a	121.0 (4)
N-C(4)-C(3)		109.8 (3)			
av	N-C_a-C_b	110.1 (5)	C(1)-C(5)-C(6)		118.7 (3)
			C(4)-C(5)-C(6)		120.2 (4)
N-C(1)-C(5)		126.2 (3)	av	C_a-C_m-C_{Me}	119.4 (11)
N-C(4)-C(5)		125.6 (4)			
av	N-C_a-C_m	125.9 (4)			

[a] The notation is that of Hoard (Hoard, J. L. *Science (Washington, D.C.)* 1971, *174*, 1295-1302). [b] Average values are weighted. In this and subsequent tables the error is taken to be the larger of the unweighted estimated standard deviation of a single observation and that estimated from the inverse matrix.

about 0.2 Å longer than that found in Ni(pc)I,[2c] Ni(tbp)I,[4] $Ni(dpg)_2I$,[29] and $Ni(bqd)_2I_{0.5}$[24] and 0.3 Å shorter than that found in $Ni(omtbp)I_{1.08}$.[6b] The stacking of the Ni(tmp) moieties in Ni(tmp)I is considerably different from the slipped stack arrangement found in the unoxidized Ni(tmp) crystal,[11a,30] where the Ni-Ni spacing is 5.648 (6) Å, and the mean plane of the Ni(tmp) molecule is inclined at an angle of approximately 36° to the stacking axis.

Ni(tmp) Molecule. A drawing of the Ni(tmp) molecule that shows the labeling scheme is presented in Figure 3. Intramolecular distances and angles are given in Table IV, and best weighted least-squares planes are given in Table V. The Ni(tmp) molecule has crystallographically imposed $\bar{4}$ (S_4) symmetry with the mean molecular plane constrained by symmetry to be $z = 0$. The pyrrole rings are essentially planar, but the molecule as a whole is nonplanar since the pyrrole rings are tilted at an angle of 12.4° with respect to the mean molecular plane. The tilting of the pyrrole rings produces a saddle shape as is apparent from Figure 4, which shows the Ni(tmp) molecule as viewed down the Ni-N bond. The angle between the planes of adjacent pyrrole

Table V. Least-Squares Planes in Ni(tmp)I

	deviations from plane, Å	
atoms	plane 1 $z = 0$	plane 2 pyrrole ring
Ni	0	0.213
N	0.101	0.014 (4)[a]
C(1)	0.043	−0.011 (6)
C(2)	0.326	−0.005 (4)
C(3)	0.547	0.014 (4)
C(4)	0.371	−0.014 (4)
C(5)	0.284	−0.241
C(6)	0.432	−0.420
C(5)		0.079
av dev	0	0.012

	plane equation: $Ax + By + Cz = D$			
plane no.	A	B	C	D
1	0	0	6.932	0
2[b]	3.377	1.178	6.769	1.515

[a] Standard deviations are given for those atoms used in the definition of the plane. [b] The dihedral angle between plane 1 and plane 2 is 12.43°.

(29) (a) Gleizes, A.; Marks, T. J.; Ibers, J. A. *J. Am. Chem. Soc.* **1975**, *97*, 3545-3546. (b) Cowie, M.; Gleizes, A.; Grynkewich, G. W.; Kalina, D. W.; McClure, M. S.; Scaringe, R. P.; Teitelbaum, R. C.; Ruby, S. L.; Ibers, J. A.; Kannewurf, C. R.; Marks, T. J. *J. Am. Chem. Soc.* **1979**, *101*, 2921-2936.

(30) Gallucci, J. C.; Swepston, P. N.; Ibers, J. A. *Acta Crystallogr., Sect. B* **1982**, *B38*, 2134-2139.

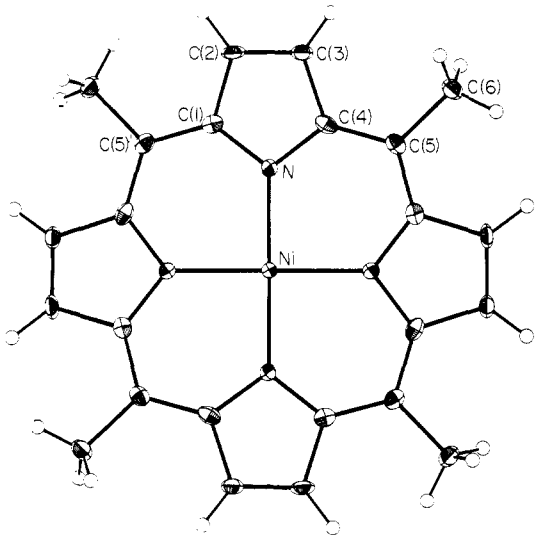

Figure 3. Drawing of the Ni(tmp) molecule with labeling scheme. Vibrational ellipsoids are drawn at the 50% probability level; hydrogen atoms are drawn arbitrarily small.

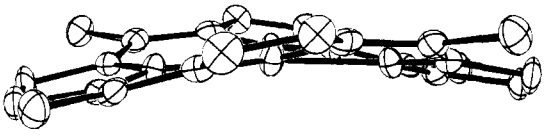

Figure 4. Ni(tmp) molecule viewed down a Ni–N bond. Hydrogen atoms have been omitted.

Table VI. Short (<3.47 Å) Intrastack Intermolecular Constants

atoms	distance, Å
Ni–Ni	3.466 (3)
N–C(4)	3.419 (6)
C(1)–C(1)	3.424 (12)
C(1)–C(5)	3.329 (8)
C(2)–C(6)	3.435 (7)

rings is approximately 17.5°, which compares well with the value of ~23° calculated[31] for the S_4-ruffled porphyrin Ni(oep) (tetragonal form)[32] and is considerably larger than the values of 2.1° and 1.9–5.2° found for the planar nickel porphyrins Ni(oep) (triclinic form)[33] and Ni(deut),[34] respectively. As a result of the puckering of the Ni(tmp) molecule, there are several non-hydrogen contacts that are shorter than the Ni–Ni separation, and these are given in Table VI.

The weighted means of chemically equivalent but crystallographically independent bond lengths and angles have been included in Table VII, along with the same data for the two other structurally characterized Ni(tmp) systems[11a,30,35] and the two crystalline modifications of Ni(oep).[32,33] The two N–C_a bond distances in Ni(tmp)I, 1.369 (5) and 1.395 (5) Å, appear to be significantly different as do the two Ni–N–C_a angles and the two C_a–C_m–C_{Me} angles, but all other chemically equivalent bond distances and angles agree well with one another. The Ni–N bond distance of 1.938 (3) Å is probably shorter than those of 1.953 (14) and 1.950 (4) Å found for the planar Ni(tmp) molecules in Ni(tmp)[11a,30] and Ni(tmp)TCNQ,[35] respectively. This shortening of the Ni–N bond length, and the concomitant decrease in the Ni–C_m distance, is a result of the central "hole" contraction that occurs when a planar porphyrin distorts to a ruffled conformation.[36] A similar decrease in the Ni–N and Ni–C_m distances was observed in going from planar to S_4-ruffled Ni(oep). An increase in the C_a–N–C_a angle and a decrease in the N–C_a–C_b angle are also expected[36] to accompany the formation of a ruffled porphyrin. These trends, which were observed in the Ni(oep) systems, are not evident in the Ni(tmp) systems. The remaining differences between the meso-substituted Ni(tmp) systems and the pyrrole-substituted Ni(oep) systems are the longer Ni–C_m distances, smaller C_a–C_m–C_a angle, and larger N–C_a–C_m angle in Ni(tmp). These differences have been observed previously in comparisons of meso- and pyrrole-substituted porphyrins[37,38] and have been attributed to steric effects of the substituent at the meso position.[38]

Disordered Iodine. The iodine atoms lie in chains along a 4-fold axis coincident with $^1/_4$, $^1/_4$, z, and the superlattice repeat of c' = 9.64 Å is typical for systems that contain one-dimensionaly disordered chains of triiodide anions.[2c,4,18–22] There are probably two causes for this type of disorder. First, disorder arises because triiodide chains in adjacent channels are shifted along z relative to one another. Second, disorder within a channel can result because steric interactions with surrounding Ni(tmp) molecules cause constrictions in the channel that partially inhibit the iodine atoms from occupying the incommensurate superlattice and force some of them to occupy the commensurate (Bragg) lattice. In this case, the iodine atoms are not randomly disordered but show a marked preference for the sites at $z = ^1/_4$ and $z = ^3/_4$ where the closest contacts between the hydrogen atoms and the channel are long (3.79 and 3.35 Å, respectively) compared with the contacts at $z = 0$ and $z = 0.5$ (3.23 Å).[39] The sites at $z = ^1/_4$ and $z = ^3/_4$ correspond to special positions (2a) and (2b), both of which have 42 (D_4) symmetry. The two sites do not have identical environments; the channel is much more constricted at $z = ^3/_4$ where the closest hydrogen atom contact is at least 0.4 Å shorter than the contact at $z = ^1/_4$. As a result, the iodine distribution centered at $z = ^1/_4$ is more dispersed than is the distribution centered at $z = ^3/_4$ as shown in Figure 1.

Stoichiometry. For Ni(tmp)I_x the value of x of 1.109 (5), derived from refinement of the X-ray data, is larger than that of 1.0, derived from the elemental analyses of single crystals from the same batch used for the X-ray studies. This disagreement may arise because we were unable to refine independently the two different iodine distributions at $z = ^1/_4$ and $z = ^3/_4$. For this reason we prefer the results from the elemental analyses and refer to the material as Ni(tmp)$I_{1.00}$.

Resonance Raman Measurements. The resonance Raman spectrum of a polycrystalline sample of Ni(tmp)I is shown in Figure 5. The room-temperature spectrum (Figure 5A) consists of a sharp peak at 105 cm^{-1} that corresponds to the totally symmetric stretching fundamental of a symmetric I_3^- anion; the characteristic overtone progression for the I_3^- anion is observed at 209, 315, and 420 cm^{-1}. This Raman scattering pattern is identical with that observed for other one-dimensional systems containing linear chains of I_3^- anions[2c,4,6b,24,40,41a] and is consistent with the results of the diffuse X-ray scattering experiment that also indicate the iodine to be present as triiodide. There is no evidence in the Raman spectrum for the presence of appreciable amounts (>2%) of I_5^- ($\nu_1 \sim$ 160–170 cm^{-1})[41] or I_2 ($\nu_1 \sim$ 180–210 cm^{-1}).[42] With a Ni(tmp):I ratio of 1:1 this compound is best

(31) Meyer (ref 32) appears to define the angle between the planes of adjacent pyrrole ring as twice the angle between the plane of one pyrrole ring and the mean molecular plane. The angle we report here is the dihedral angle between the planes of two adjacent pyrrole rings as calculated from the atomic coordinates given in ref 32.

(32) Meyer, E. F., Jr. *Acta Crystallogr., Sect. B* **1972**, *B28*, 2162–2167.

(33) Cullen, D. L.; Meyer, E. F., Jr. *J. Am. Chem. Soc.* **1974**, *96*, 2095–2102.

(34) Hamor, T. A.; Caughey, W. S.; Hoard, J. L. *J. Am. Chem. Soc.* **1965**, *87*, 2305–2312.

(35) Pace, L. J.; Ulman, A.; Ibers, J. A. *Inorg. Chem.* **1982**, *21*, 199–207.

(36) Hoard, J. L. *Ann. N.Y. Acad. Sci.* **1973**, *206*, 18–31.

(37) Lauher, J. W.; Ibers, J. A. *J. Am. Chem. Soc.* **1973**, *95*, 5148–5152.

(38) Cullen, D. L.; Meyer, E. F., Jr. *Acta Crystallogr., Sect. B* **1973**, *B29*, 2507–2515.

(39) All of the calculated hydrogen atom to channel contacts are longer than the sum of the van der Waals' radii of hydrogen and iodine, 3.15 Å. If this were truly the case, none of the contacts would be short enough to cause a modulation of the iodine electron density, and the disorder would be completely random. However, the value of 0.95 Å used for the C–H bond length in the solution of the structure is an underestimation of the C–H internuclear separation, so the actual hydrogen–iodine contacts are undoubtedly shorter than the calculated values.

(40) Trotter, P. J.; White, P. A. *Appl. Spectrosc.* **1978**, *32*, 323–324.

(41) (a) Marks, T. J., in ref 8a; pp 594–616. (b) Teitelbaum, R. C.; Ruby, S. L.; Marks, T. J. *J. Am. Chem. Soc.* **1978**, *100*, 3215–3217.

Table VII. Averaged Bond Lengths (Å) and Angles (deg) of Ni(tmp) and Ni(oep) Systems

bond parameter	Ni(tmp)[a]	Ni(tmp)TCNQ[b]	Ni(tmp)I[c]	triclinic Ni(oep)[d]	tetragonal Ni(oep)[e]
Ni–N	1.953 (14)[f]	1.950 (4)	1.938 (3)	1.958 (2)	1.929 (3)
N–C_a	1.384 (3)	1.388 (6)	1.381 (18)	1.376 (6)	1.386 (4)
C_a–C_b	1.439 (3)	1.435 (6)	1.446 (5)	1.444 (4)	1.449 (5)
C_b–C_b	1.334 (5)	1.339 (6)	1.339 (6)	1.346 (4)	1.326 (5)
C_a–C_m	1.378 (2)	1.380 (6)	1.388 (11)	1.372 (4)	1.373 (5)
Ni–C_m	3.422 (2)	3.429 (4)	3.410 (5)	3.381 (3)	3.355 (4)
N–Ni–N	90.00 (4)	90.0 (1)	90.16 (1)	90.15 (9)	90.0 (1)
Ni–N–C_a	127.6 (3)	127.7 (3)	127.3 (7)	128.0 (2)	127.4 (2)
C_a–N–C_a	104.8 (4)	104.6 (3)	105.2 (3)	104.0 (4)	105.1 (3)
N–C_a–C_b	110.2 (2)	110.3 (4)	110.1 (5)	111.6 (3)	110.6 (2)
N–C_a–C_m	126.3 (3)	126.5 (4)	125.9 (4)	124.4 (3)	124.0 (2)
C_a–C_b–C_b	107.4 (1)	107.4 (5)	107.2 (5)	106.5 (4)	106.8 (3)
C_b–C_a–C_m	123.5 (4)	123.2 (6)	123.6 (4)	124.1 (4)	125.0 (2)
C_a–C_m–C_a	121.9 (1)	121.4 (5)	121.0 (4)	125.2 (3)	124.1 (2)
C_a–C_m–C_{Me}	119.1 (10)	119.3 (7)	119.4 (11)		

[a] Reference 30; 139 K. [b] Reference 35; 116 K. [c] This work; 114 K. [d] Reference 33; 298 K. [e] Reference 32; 298 K. [f] The estimated standard deviation of a single observation is given in parentheses. A possible explanation for the significantly unequal Ni–N distances in Ni(tmp) is given in Kutzler et al. (Kutzler, F. W.; Swepston, P. N.; Berkovitch-Yellin, Z.; Ellis, D. E.; Ibers, J. A. *J. Am. Chem. Soc.*, in press).

formulated as $[Ni(tmp)]^{0.33+}(I_3^-)_{0.33}$, where 1 electron per three Ni(tmp) molecules has been transferred to one I_3^- counterion.

The low-temperature (10 K) spectrum of Ni(tmp)I is shown in Figure 5B, along with the low-temperature spectrum of Ni(tbp)I, a system that also has been found[4] to contain iodine in the form of I_3^-. The recording of both spectra was accompanied by the slow decomposition of the samples in the laser beam,[43] as indicated by the growth of bands around 190 cm^{-1} assignable to the I_2 symmetric stretching fundamental. This fundamental is present in the spectrum of Ni(tmp)I as a doublet with peaks at 181 and 190 cm^{-1}; a similar splitting of an I_2 fundamental was observed in the resonance Raman spectrum of crystalline I_2 (ν_1 = 180, 188 cm^{-1})[44] at 30 K and was attributed to correlation field effects (factor group splitting). The decomposition of the I_3^- anion to I_2 (and, depending on the stoichiometry of the reaction, possibly to I^- which is not detectable by resonance Raman spectroscopy) does not appear to alter the major feature seen in the room-temperature spectrum, namely the symmetric stretching fundamental and overtone progression of I_3^-. At 10 K, however, these bands sharpen considerably, and in the spectrum of Ni(tmp)I, a splitting of approximately 4 cm^{-1} is evident, with ν_1 = 107, 111 cm^{-1} and $2\nu_1$ = 216, 220 cm^{-1}. The remaining overtones, which have not been included in Figure 5B, are weak and broad. As is true for the I_2 stretching mode, the splitting of the I_3^- band may well be the result of correlation splitting; however, our understanding of the composition of the iodine supercell is too limited to allow us to carry out a detailed factor group analysis of this system.

On the other hand, as discussed below, susceptibility measurements show that Ni(tmp)I undergoes a transition at 28 K. It may be that the doubling of the Raman peaks at 10 K reflects a structural change that occurs at the transition. This suggestion receives some support when related systems are considered. There are no splittings in the low-temperature spectra of Ni(tbp)I (Figure 5B), Ni(pc)I,[2c] Ni(tatbp)I,[3] and M(dpg)$_2$I (M = Ni, Pd).[29b] None of these systems exhibits a sharp low-temperature transition. Splitting of I_3^- bands has been observed previously, however, in the resonance Raman spectra taken at 108 K of $[(C_4H_9)_4N]I_3$ and $[(C_2H_5)_4N]I_3$,[45] where the two component peaks of the I_3^- symmetric stretching fundamental are separated by 7 and 0.8 cm^{-1}, respectively, as well as in the conducting linear chain system $DIPSPh_4(I_3^-)_{0.76}$,[46] with a splitting of 7 cm^{-1}. In the latter case the splitting occurs only in the low iodine content, highly conducting phase and is attributed to pairwise interaction of I_3^- ions in a column.

Magnetic Measurements. Crystals of Ni(tmp)I exhibit a single, narrow EPR signal that has an angle-dependent g value and line width. An analysis of this signal provides information on the type of orbital (i.e., Ni^{III} d orbital, tmp^+ π orbital, or a d–π mixture) that loses the electron upon oxidation of the Ni(tmp) molecule, while susceptibility measurements provide a means of characterizing the interactions that occur between the Ni(tmp) molecules in the partially oxidized stack.

(i) EPR *g* Values. The angle dependence for an axially symmetric g tensor is described by

$$g(\theta) = [g_\parallel^2 \cos^2\theta + g_\perp^2 \sin^2\theta]^{1/2} \quad (2)$$

where θ is the angle between the applied magnetic field and the unique tensor axis, c. A least-squares fit to eq 2 of the experimental data for Ni(tmp)I gives values of $g_\parallel$ = 2.0067 (2) and $g_\perp$ = 2.0024 (2). Both $g_\parallel$ and $g_\perp$ are very close to the free-electron value (g_e = 2.0023) as expected for a ligand-centered oxidation (i.e., formation of $[Ni^{II}(tmp^+)]$); metal-centered oxidation would give g values much larger than g_e.[47] The narrow line widths observed for Ni(tmp)I (vide infra) also are consistent with the formation of a π-cation radical. Thus, the best formulation for Ni(tmp)I is $[Ni(tmp)^+][Ni(tmp)]_2(I_3^-)$, or $[Ni^{II}(tmp)]^{0.33+}(I_3^-)_{0.33}$.

For a π-cation radical, we expect $g_\perp > g_\parallel \sim g_e$, while for Ni(tmp)I we find $g_\parallel > g_\perp \sim g_e$. This behavior has been observed previously in the ligand-oxidized $Ni(omtbp)I_{1.08}$[6b] and Ni(pc)I[2c] systems and has been attributed to the existence of a small fraction of the hole density on the iodine chain. Back-transfer of charge from I_3^- to the macrocyclic stack causes an increase in $g_\parallel$ and a small decrease in $g_\perp$.[6b] From the measured $g_\parallel$ value of 2.0067 and formulas previously obtained,[6b] we calculate the degree of back-charge-transfer to be 0.002. This value is identical with that found for Ni(pc)I[2c] and is slightly lower than the value of 0.004 found for $Ni(omtbp)I_{1.08}$.[6b] As was true for Ni(pc)I and $Ni(omtbp)I_{1.08}$, the g values for Ni(tmp)I remain constant within experimental error from room temperature down to 4.2 K. Thus, we infer that the electronic structure of Ni(tmp)I does not change significantly with temperature.

(ii) EPR Line Widths. The EPR line shape of single crystals of Ni(tmp)I for all orientations is roughly Lorentzian at room temperature and remains so down to 4.2 K. At room temperature the peak-to-peak derivative line width Γ is axially symmetric with an angle dependence of

$$\Gamma(\theta) = \Gamma_0 + \Gamma_1(1 + \cos^2\theta) \quad (3)$$

which has been fit with Γ_0 = 7.31 G and Γ_1 = −1.34 G (Figure

(42) Kiefer, W. *Appl. Spectrosc.* **1974**, *28*, 115–133.
(43) Local heating by the laser beam causes the decomposition of the sample. At the present time this problem is unavoidable because it is not possible to spin the sample in our low-temperature apparatus, and the evacuated sample chamber does not permit efficient heat transfer away from the sample.
(44) Anderson, A.; Sun, T. S. *Chem. Phys. Lett.* **1970**, *6*, 611–616.
(45) Gabes, W.; Gerding, H. *J. Mol. Struct.* **1972**, *14*, 267–279.
(46) Faulques, E.; Rzepka, E.; Lefrant, S.; Strzelecka, S. *Mol. Cryst. Liq. Cryst.* **1982**, *86*, 63–69.
(47) Wolberg, A.; Manassen, J. *Inorg. Chem.* **1970**, *9*, 2365–2367.

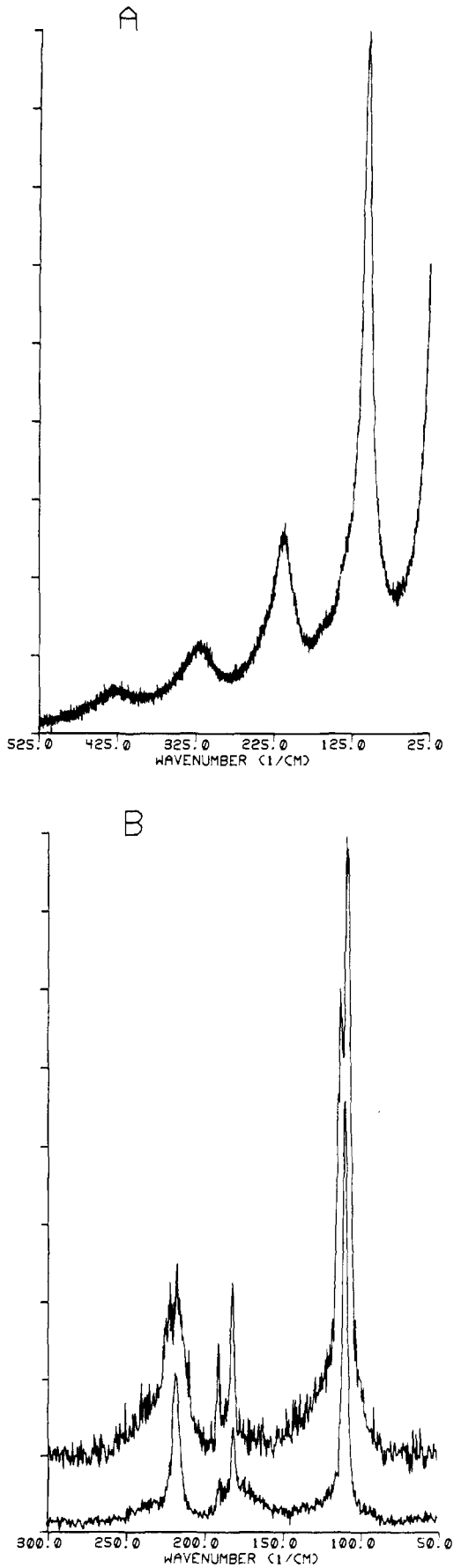

Figure 5. Resonance Raman spectra (5145-Å excitation) of polycrystalline samples of (A) Ni(tmp)I at room temperature and (B) Ni(tmp)I (upper) and Ni(tbp)I (lower) at 10 K. The wavelength scale of (B) is expanded relative to that of (A) to emphasize the splitting of the bands in the low-temperature spectrum of Ni(tmp)I.

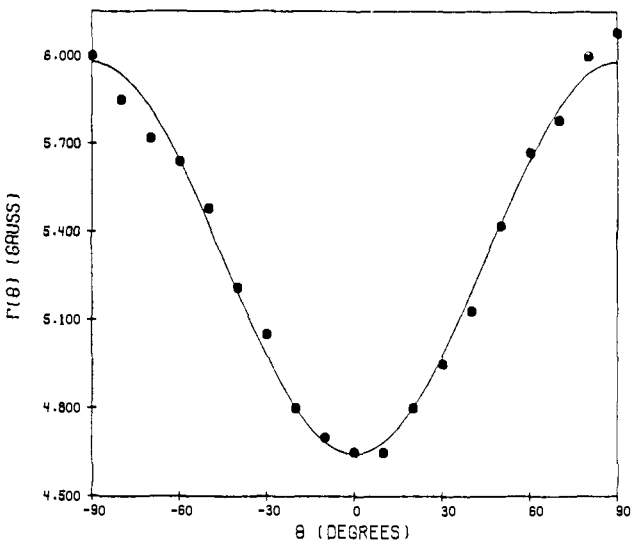

Figure 6. Angular dependence of the EPR line width at room temperature for Ni(tmp)I. The solid line is the theoretical fit to eq 3.

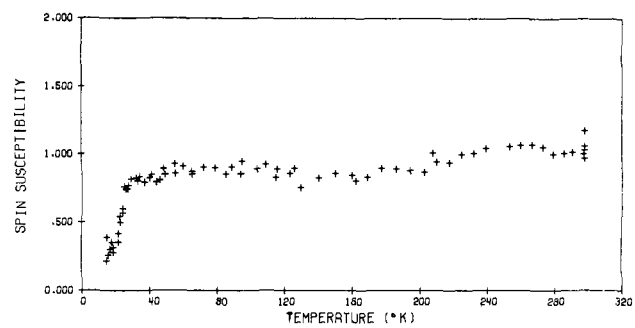

Figure 7. Temperature dependence of the normalized spin susceptibility ($\chi(T)/\chi(298\ K)$) for a single crystal of Ni(tmp)I oriented with the c axis perpendicular to the magnetic field.

6). The functional form of eq 3, but with $\Gamma_1 > 0$, has been discussed[2,6b] in terms of electron spin dipole–dipole interactions that are exchange narrowed.[48] The angular dependence with $\Gamma_1 < 0$, which is rarer but has been observed in several other porphyrinic conductors as well,[49,50] has yet to be explained. The line width decreases with decreasing temperature down to 50 K. Below this temperature the line is very narrow ($\Gamma \leq 0.3$ G) and temperature independent. The anisotropy also decreases on cooling, with the signal becoming essentially isotropic by 120 K. This type of behavior is very similar to that observed for $Ni(omtbp)I_{1.08}$[6b] and $(TTT)_2I_3$.[51] In the former case the temperature variation was shown to result from the temperature dependence of correlated hopping of charge carriers along the Ni(omtbp) stacks; however, in general this behavior is imperfectly understood.

(iii) Susceptibility. The measured room-temperature static susceptibility of a powder sample of Ni(tmp)I is $\chi = 0.78 \times 10^{-4}$ emu/mol. When this value is corrected for the temperature-independent diamagnetism ($\chi^d = -2.85 \times 10^{-4}$ emu/mol from Pascal's constants), the paramagnetic susceptibility is calculated to be $\chi^P = 3.63 \times 10^{-4}$ emu/mol; this value corresponds to 0.29 (2) $S = {}^1/_2$, $g = 2$ spins per macrocycle. From absolute EPR intensity measurements, we find a spin susceptibility that corresponds to 0.31 (3) spins per macrocycle, in good agreement with the static susceptibility results.

The spin susceptibility for a single crystal of Ni(tmp)I (Figure 7) is isotropic and essentially temperature independent down to

(48) Soos, Z. G.; Huang, T. Z.; Valentine, J. S.; Hughes, R. C. *Phys. Rev. B: Solid State* **1973**, *8*, 993–1001.
(49) Schramm, C. J.; Martinsen, J.; Palmer, S. M.; Hoffman, B. M., manuscript in preparation.
(50) Martinsen, J.; Phillips, T. E.; Hoffman, B. M., unpublished results.
(51) Delhaes, P. In "The Physics and Chemistry of Low-Dimensional Solids"; Alcacer, L., Ed.; D. Reidel: Boston, MA, 1980; pp 281–291.

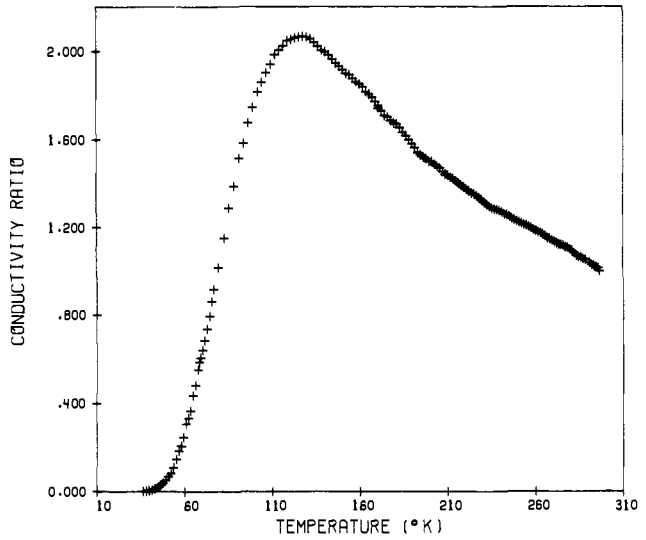

Figure 8. Temperature dependence of the normalized conductivity ($\sigma_{\parallel}(T)/r_{\parallel}$(298 K)) along the needle (c) axis of a single crystal of Ni(tmp)I.

a transition temperature of 28 K. Below the transition the susceptibility decrease is roughly described as an activated process ($\chi T \sim (\exp(-\Delta/(kT)) + 3)^{-1}$), with an activation energy $\Delta/k \sim 60$ cm^{-1}. Further work will be needed to characterize better the magnetic behavior in the vicinity of the transition temperature.

In the Ni(tbp)I[4] and Ni(pc)I[2c] systems, where the measured paramagnetism is low (~0.1 spins per macrocycle compared with the value of 0.33 expected from the ionicity), the observed temperature-independent susceptibility was described as Pauli-like and for illustrative purposes was modeled in terms of a tight-binding band of noninteracting electrons. Clearly, it is not appropriate to describe the temperature-independent susceptibility of Ni(tmp)I (30 K $\leq T \leq$ 298 K) in this fashion because the room-temperature paramagnetism is as high ($\sim^1/_3$ spin per macrocycle) as would be observed for noninteracting carrier spins. The organic conductors $(TMTTF)_2X$, X = ClO_4^-, BF_4^-[10] exhibit magnetic behavior that is very similar to that of Ni(tmp)I, with both a high room-temperature paramagnetism and roughly temperature-independent susceptibility accompanied by a low-temperature transition to a diamagnetic state.

Electrical Conductivity. The room-temperature value of the electrical conductivity along the needle axis of single crystals of Ni(tmp)I ranges with crystal from 40 to 270 Ω^{-1} cm^{-1}, with an average value of 110 Ω^{-1} cm^{-1}. This is comparable with the value for Ni(tbp)I (150–330 Ω^{-1} cm^{-1})[4] and is slightly lower than that of Ni(pc)I (260–750 Ω^{-1} cm^{-1})[2b] or of the organic metals,[8] and an order of magnitude larger than that of the polaronic conductor $Ni(omtbp)I_{1.08}$ (4–16 Ω^{-1} cm^{-1}).[6] A more instructive comparison employs the carrier mean free path, $\bar{\lambda}_{\parallel}$, obtained within the framework of one-electron tight-binding band theory and expressed in units of the intermolecular spacing in the conducting stack. A value of $\bar{\lambda}_{\parallel} > 1$ indicates that conduction is significantly wavelike, while $\bar{\lambda}_{\parallel} < 1$ is generally associated with a diffusing or hopping conductor. For the best Ni(tmp)I crystals, $\bar{\lambda}_{\parallel} \sim 0.5$, in comparison with values of 1.0–2.3 for Ni(pc)I,[2c] 0.7–1.3 for Ni(tbp)I,[4] and 0.04 for $Ni(omtbp)I_{1.08}$.[6b]

The temperature dependence of the electrical conductivity of Ni(tmp)I (Figure 8) is characteristic of quasi one-dimensional molecular conductors, both organic and inorganic.[8] At high temperatures, the crystal exhibits metallic conductivity ($d\sigma/dT < 0$) along the one-dimensional stack. The curve in this region follows the usual form associated with a temperature-dependent carrier mobility, $\sigma(T) \propto T^{-\beta}$; in this case $\beta = 0.9$–1.1. Molecular conductors typically show a steeper rise, with values for β ranging from 2 to 4,[52] although β is approximately 1 for Ni(tbp)I, and is unity for true metals. The conductivity reaches a maximum of approximately twice the room-temperature value at a temperature $T_m \sim 115 \pm 10$ K. This conductivity corresponds to $\bar{\lambda}_{\parallel} \sim 1$, the nominal dividing line between diffusive and wave-like conductivity. The value of T_m is sample-dependent, those crystals with the highest conductivity having the lowest T_m. At temperatures below T_m, $\sigma(T)$ decreases rapidly. In all cases the crystals can be thermally cycled with no evidence of hysteresis or sample degradation. The data in the temperature region between 35 and 80 K have been fit to a thermally activated temperature dependence with an activation energy of 0.037 eV. This value falls within the range reported for organic conductors.[57]

The transition from metallic conductivity, through a broad maximum, to semiconducting behavior is thought to arise from either or both of two mechanisms peculiar to one-dimensional conductors. The first is the Peierls instability, an inherent tendency of a regular (equally spaced) conducting stack to undergo a periodic distortion that lowers the crystal free energy but abolishes the high-temperature metal-like conductivity and introduces an activation energy for conduction.[8c,53] In some cases distortions along individual chains interact and lock together to give a true three-dimensional and sharp phase transition. The second factor arises from the chemistry rather than the physics of these one-dimensional materials. Random potentials,[54,55] such as those created by the structurally disordered I_3^- chains of Ni(tmp)I or by imperfections,[56,57] tend to localize the wave functions on a conducting stack at low temperatures.[55]

Discussion

Partial oxidation with iodine of the small-ring porphyrin Ni(tmp) results in the compound Ni(tmp)I, which may be formulated as the partially ring-oxidized system $[Ni(tmp)^{0.33+}](I_3^-)_{0.33}$. This material has the same ionicity and the same type of charge carriers (electron "holes" on the ring) as do several of its large-ring counterparts, and the magnitude and temperature response of the conductivity in the two classes of compounds are comparable.[2-4] The large-ring M(L)I compounds, Ni(pc)I, Ni(tatbp)I, and Ni(tbp)I, exhibit paramagnetic susceptibilities that are very much like those of a metal, namely a very weak temperature dependence, and a room-temperature value strongly reduced from that expected for noninteracting radicals. In this context the susceptibility of Ni(tmp)I is anomalous: above 28 K it varies less with temperature than that of any of the other iodinated compounds and thus appears highly metal-like, yet it is roughly 3 times larger in magnitude. Indeed, at room temperature the value of χ corresponds to one Ni(tmp) cation spin per triiodide anion, essentially that of noninteracting spins. We first recall the theoretical framework for describing the susceptibility of a one-dimensional conductor and then analyze this striking difference between Ni(tmp)I and the other porphyrinic systems.

The weakly temperature-dependent susceptibility of a quasi-one-dimensional molecular conductor is frequently discussed in terms of a theory, called the tight-binding model,[8c] that is formally identical with the Hückel theory for an infinite regular polyene. An odd-electron (hole) in the HOMO of an oxidized M(L) unit in a molecular stack is mobile because of the intersite interaction, which is written in terms of an electron-transfer matrix element, t, called β in Hückel theory. For a chain of N sites, $N \rightarrow \infty$, the localized single-site orbitals become a dense band of delocalized states having a bandwidth of $4t(4\beta)$. This model predicts that

(52) (a) Epstein, A. J.; Conwell, E. M.; Sandman, D. J.; Miller, J. S. *Solid State Commun.* **1977**, *23*, 355–358. (b) Epstein, A. J., in ref 8d; pp 155–161.

(53) Kittel, C. "Introduction to Solid State Physics"; Wiley: New York, 1976.

(54) Barland, R. E. *Proc. Phys. Soc., London* **1961**, *78*, 926–931.

(55) (a) Bloch, A. N.; Weisman, R. B.; Varma, C. M. *Phys. Rev. Lett.* **1972**, *28*, 753–756. (b) Gruner, G.; Janossy, A.; Holczer, K.; Mihaly, G., in ref 8f; pp 246–254. (c) Epstein, A. J.; Miller, J. S., in ref 8f; pp 265–272. (d) Epstein, A. J.; Conwell, E.; Miller, J. S., in ref 8a; pp 183–208.

(56) (a) Kuse, D.; Zeller, H. R. *Phys. Rev. Lett.* **1971**, *27*, 1060–1063. (b) Rice, M. J. *Phys. Lett. A* **1972**, *39A*, 289–290. (c) Rice, M. J.; Bernasconi, J. *Phys. Lett.* **1972**, *38*, 277–278. (d) Rice, M. J.; Bernasconi, J. *J. Phys. F* **1973**, *3*, 55–66.

(57) (a) Sheng, P.; Sichel, E. K.; Gittleman, J. I. *Phys. Rev. Lett.* **1978**, *40*, 1197–1200. (b) Sheng, P. *Phys. Rev. B* **1980**, *21*, 2180–2195.

the magnitude of the susceptibility of the compound is inversely proportional to the bandwidth and that the temperature dependence of the susceptibility also diminishes with increasing bandwidth. The susceptibility of Ni(tmp)I, which is large at room temperature but is temperature invariant, cannot be accommodated within this simplified model.[58] The failure of the model most probably arises because it neglects electron correlation effects, a defect which leads to a problem well-known to chemists in the context of one-electron molecular orbital theories: overemphasis of "ionic" states. The many-electron tight-binding wave function includes not only terms with oxidized $Ni(L)^+$ and neutral Ni(L) molecules but also has contributions from doubly oxidized $Ni(L)^{2+}$ sites. Since such dicationic sites typically are closed shell and diamagnetic, they contribute to the susceptibility reduction in the metallic state. However, dicationic sites are energetically unfavorable by roughly the difference between the first and second ionization (or redox) potentials of Ni(L). This disproportionation energy is equivalent to a correlation or repulsion energy between holes[59-62] and has been given the symbol U.

Correlation effects are addressed in a treatment known as the Hubbard model,[59] whose operational parameter is the ratio of the correlation energy to the bandwidth: $U/4t$. As this ratio increases, the closed shell, diamagnetic dicationic terms are suppressed, with a resultant increase in the magnitude of the magnetic susceptibility. In addition, the holes are increasingly forced to avoid each other and behave more as independent paramagnets with the result that the susceptibility becomes more strongly temperature dependent.

In the large-ring systems Ni(pc)I[2c] and Ni(tbp)I,[4] the susceptibility looks very much like that of a metal, being reduced and nearly temperature independent, and thus in these systems delocalization effects are comparable to or greater than hole repulsion: $U/4t \ll 1$. The system $Ni(omtbp)I_{1.08}$[6] represents the limit, referred to as the atomic limit, in which delocalization along a stack is weak, and therefore Coulomb interactions dominate: $U/4t \rightarrow \infty$. This limit is realized because structural features reduce t. The Ni(omtbp) subunits of the conducting stack are roughly the same size as the subunits in the better molecular metals Ni(pc)I and Ni(tbp) and likely have a comparable value for U, but the spacing between the Ni(omtbp) units in the conducting stack is large, reducing intermolecular overlaps. Indeed, the susceptibility of $Ni(omtbp)I_{1.08}$ obeys the Curie law, indicative of a delocalization interaction $t < 3\ cm^{-1}$. As a result, correlation effects dominate, the charge carriers are highly localized, and conduction is by a hopping process.[6c]

The properties of Ni(tmp)I place it in an intermediate position in terms of the relative importance of delocalization (t) and correlation (U) effects. In particular, weak temperature dependence of the susceptibility is indicative of significant delocalization, whereas its large room-temperature value results from correlation effects. That both delocalization and correlation effects are important can be qualitatively understood in terms of the structure of Ni(tmp)I and the properties of the parent metallomacrocycle.

We expect t to be proportional to the intermolecular, intrastack overlap, varying directly with the number of close atom–atom overlaps and inversely with the size of the ring and the average intermolecular distance, d. Thus, t for Ni(tmp)I (d = 3.48 Å) should be smaller than for Ni(pc)I and Ni(tbp)I (d = 3.24 Å) but substantially larger than for $Ni(omtbp)I_{1.08}$ (d = 3.78 Å). In addition, U, which is the repulsion between like charges, we expect to be larger in Ni(tmp)I than in any of the large-ring systems simply because the charge on Ni(tmp)I is less delocalized (a smaller "box"). Therefore, simple considerations support the conclusion that the value of $U/4t$ for Ni(tmp)I is intermediate between that of Ni(pc)I and $Ni(omtbp)I_{1.08}$ because of both intra and intermolecular features of the compound.

Thus, it would seem that Ni(pc)I, Ni(tmp)I, and Ni(omtbp)I form an isoionic series in which Coulomb correlations (U) are of progressively greater importance relative to charge-transfer interactions (t):

$$\infty \xleftarrow[U/4t]{\text{Ni(omtbp)I} \quad \text{Ni(tmp)I} \quad \text{Ni(pc)I}} 0$$

and that the *relative* importance of the correlation effects in these and other metalloporphyrins can be modified through changes in the metallomacrocycle building blocks.

The unique electronic structure[63] of the small-ring porphyrins has led us to consider an additional mechanism by which the susceptibility of Ni(tmp)I could be enhanced through contributions from an energetically accessible, open-shell dicationic state. In contrast to all other molecules that form the basis of a conductive molecular crystal, both organic and inorganic, the small-ring porphyrinic complexes need not have a single, nondegenerate HOMO; rather the two highest occupied molecular orbitals of metalloporphyrins are nearly degenerate. Simple arguments of the Hund's rule type show that an open-shell dication of such a molecule will be lower in energy than a closed-shell dication for a comparable nondegenerate molecule. Thus, creation of a dication is facilitated. However, the most stable dication state will be a triplet, not a singlet as for a closed-shell dication, and any quantum mechanical contribution to the crystal wave function would lead directly to a susceptibility enhancement. Quantum chemical calculations should be able to test this possibility.

Acknowledgment. We thank Dr. William B. Euler and Professor Mark A. Ratner for many helpful discussions. This work has been supported under the NSF-MRL program through the Materials Research Center of Northwestern University (Grant DMR79-23573) and by the National Science Foundation Grants DMR77-26409 to B.M.H. and CHE80-09671 to J.A.I. L.J.P. acknowledges receipt of an NSF Graduate Fellowship, and A.U. thanks the Minna-James-Heineman-Stiftung for financial assistance.

Supplementary Material Available: Table III (the root-mean-square amplitudes of vibration) and the listing of observed and calculated structure amplitudes (6 pages). Ordering information is given on any current masthead page.

(58) Torrance, J. B.; Tomkiewicz, Y.; Silverman, B. D. *Phys. Rev. B* **1977**, *15*, 4738–4749.
(59) Hubbard, J. *Proc. R. Soc. London, Ser. A* **1963**, *276*, 238–257; **1963**, *277*, 237–259; **1964**, *281*, 401–419.
(60) Shiba, H. *Phys. Rev. B: Solid State* **1972**, *6*, 930–938.
(61) The temperature dependence of the susceptibility in the mathematically complex regime of $U \sim 4t$ was not considered in ref 58 and 60.
(62) Mazumdar, S.; Soos, Z. G. *Synth. Met.* **1979**, *1*, 77–94.
(63) Gouterman, M. In "The Porphyrins"; Dolphin, D., Ed.; Academic Press: New York, 1978; Vol. III, pp 1–165.